Supporting Information

Suppression of low-frequency electronic noise in polymer nanowire field-effect transistors

Francesca Lezzi,[†,‡] Giorgio Ferrari,[¶] Cecilia Pennetta, [†,††] and Dario Pisignano[†,‡,¶¶,]*

[†] Dipartimento di Matematica e Fisica "Ennio De Giorgi", Università del Salento, via Arnesano I-73100 Lecce, Italy

[‡] Center for Biomolecular Nanotechnologies @UNILE, Istituto Italiano di Tecnologia, Via Barsanti, I-73010 Arnesano (LE), Italy

[¶] Dipartimento di Elettronica, Informazione e Bioingegneria, Politecnico di Milano, Via Colombo 81, I-20133 Milano, Italy

[††] INFN, Istituto Nazionale di Fisica Nucleare, Via Sansone 1, I-50019 Sesto Fiorentino (FI), Italy

[¶¶] Istituto Nanoscienze-CNR, Euromediterranean Center for Nanomaterial Modelling and Technology (ECMT), via Arnesano, I-73100 Lecce, Italy

* dario.pisignano@unisalento.it

1. Geometrical dependence of the noise

Following the analysis proposed by Lai *et al.*,[S1] we have studied the dependence of the noise from the geometry of the device in order to discriminate effects dominated by the conductive channel and noise limited at the contact region. For a transistor operating in linear regime and assuming the Hooge model, the noise as a function of the power dissipation $V_{SD} \cdot I_D$ is proportional to $1/L^2$ and independent of the effective channel width, Z, as shown by the Eq. 2 of the main text. In the case of a not negligible effect of the contact resistance and/or of the noise in the contact region, the noise scales with a different power of L and depends also by the charge injection width at the contact, as summarized in Table S1. Here, the various regimes are considered by taking into account the following approximations:

(i) for $R_{CH} > R_C$: $\frac{S_I}{V_{DS} I_{DS}} \sim \frac{S_I}{R_{CH} I_{DS}^2} \sim \frac{Z S_I}{L I_{DS}^2}$;

(ii) for $R_{CH} < R_C$: $\frac{S_I}{V_{DS} I_{DS}} \sim \frac{S_I}{R_C I_{DS}^2} \sim \frac{Z S_I}{I_{DS}^2}$.

Figure S1 shows the noise for devices with different channel length, L. The width of the used electrodes is W = 100 μm for devices with L = 25 μm, and varied up to W = 3 mm for devices with L = 6 μm and L= 12 μm.

Condition	Noise normalized by the power dissipation: $\frac{S_I}{V_{DS} I_{DS}}$
$R_{CH} > R_C$ $S_{RCH} > S_{RC}$	$\propto \frac{1}{L^2}$
$R_{CH} > R_C$ $S_{RCH} < S_{RC}$	$\propto \frac{Z^2}{L^3}$
$R_{CH} < R_C$ $S_{RCH} > S_{RC}$	$\propto L$
$R_{CH} < R_C$ $S_{RCH} < S_{RC}$	$\propto Z^2$

Table S1. Relationship between the total noise and the geometry of the device in various operation conditions. R_{CH}: resistance of the conductive channel ($\propto L/Z$). R_C: resistance at the contacts ($\propto Z^{-1}$). The total flicker noise is modeled by the sum of two uncorrelated terms, related to the channel (S_{RCH}) and to the contacts (S_{RC}), respectively. See reference S1 for additional details.

The noise at $V_{DS}I_D$ =1 μW as a function of the device length is reported in Figure S2. Here, noise is normalized by the square of the device length to highlight the dependence on this parameter. Devices with channel length of 6 μm and 12 μm and W = 1-3 mm show a noise roughly proportional to $1/L^2$ (with $S_I L^2/V_{DS}I_{DS} \cong$ 2-6×10^{-28} A^{2}m^2/W Hz) consistently with a noise source dominated by the organic semiconductor in the channel. The results are analogous for nanofibers and for thin-film OFETs. On the contrary, nanofiber-based OFETs having L= 25 μm and W = 100 μm show a noise up to two orders of magnitude lower than the other devices ($S_I L^2/V_{DS}I_{DS} \cong 5\times10^{-30}$ A^{2}m^2/W Hz). The result strongly suggests that some effects are taking place at the contact region for these devices, possibly leading contact resistance to be comparable with or to dominate over the contribution of the channel. The correlation of an overall reduced noise and a significantly increased contact resistance is also in

agreement with the model developed here as detailed in the next Section. Indeed, in devices with miniaturized electrodes (W = 100 μm), Cr/Au bonding pads are very close to the conductive channel of the transistors. Hence, this geometry leads to possible spurious effects due to wire bonding needed for device characterization. Overall, these various classes of devices allow different effects and operation conditions (i.e., $R_{CH} > R_C$ or $R_{CH} \leq R_C$) to be reliably discriminated.

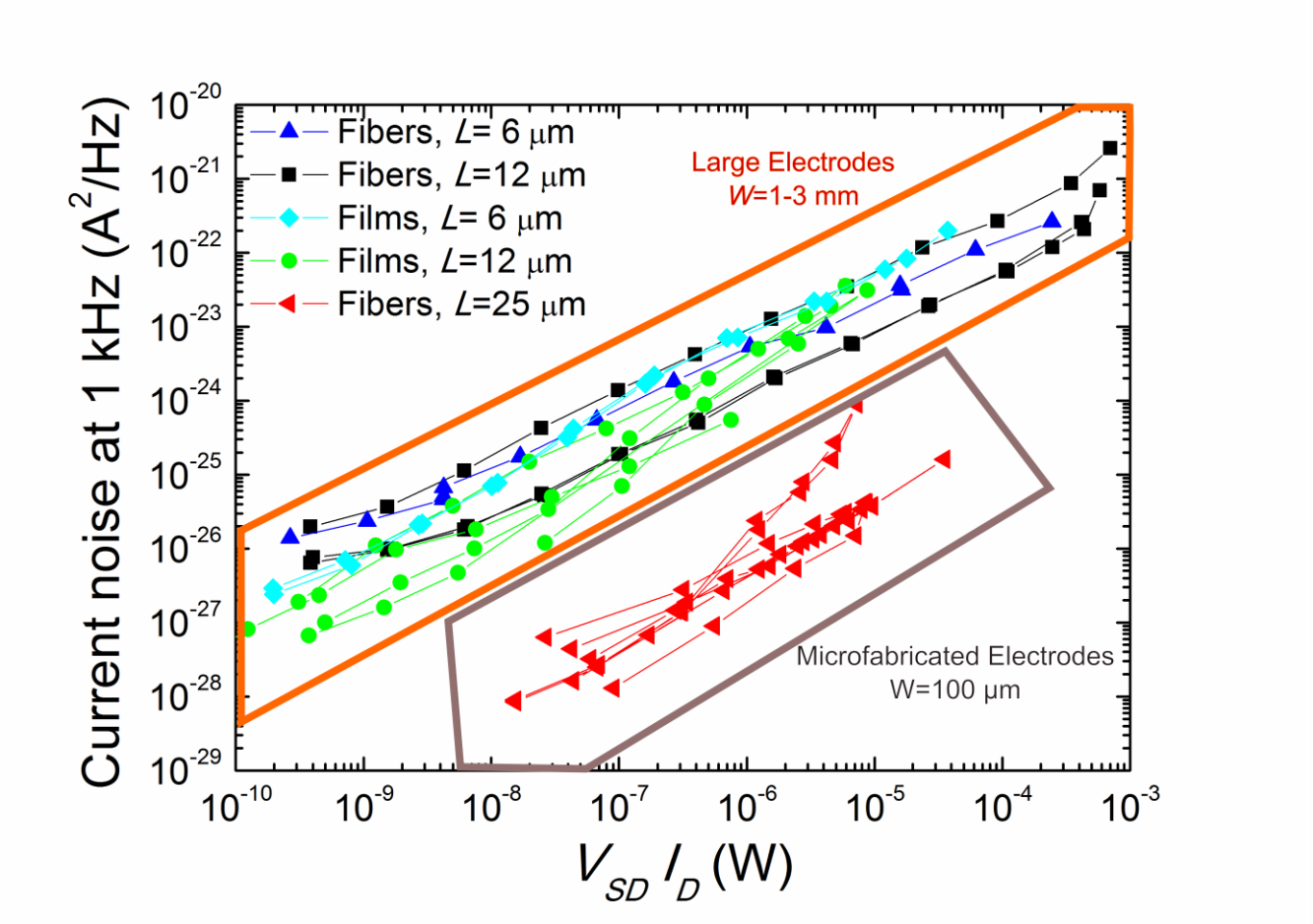

Figure S1. Noise level at 1 kHz, for a set of devices with different channel lengths and widths, and different geometries of electrodes as highlighted by the different regions of the plot. The circles and diamonds refer to OFETs based on thin-films. Devices with L= 25 μm embed miniaturized (W = 100 μm) electrodes.

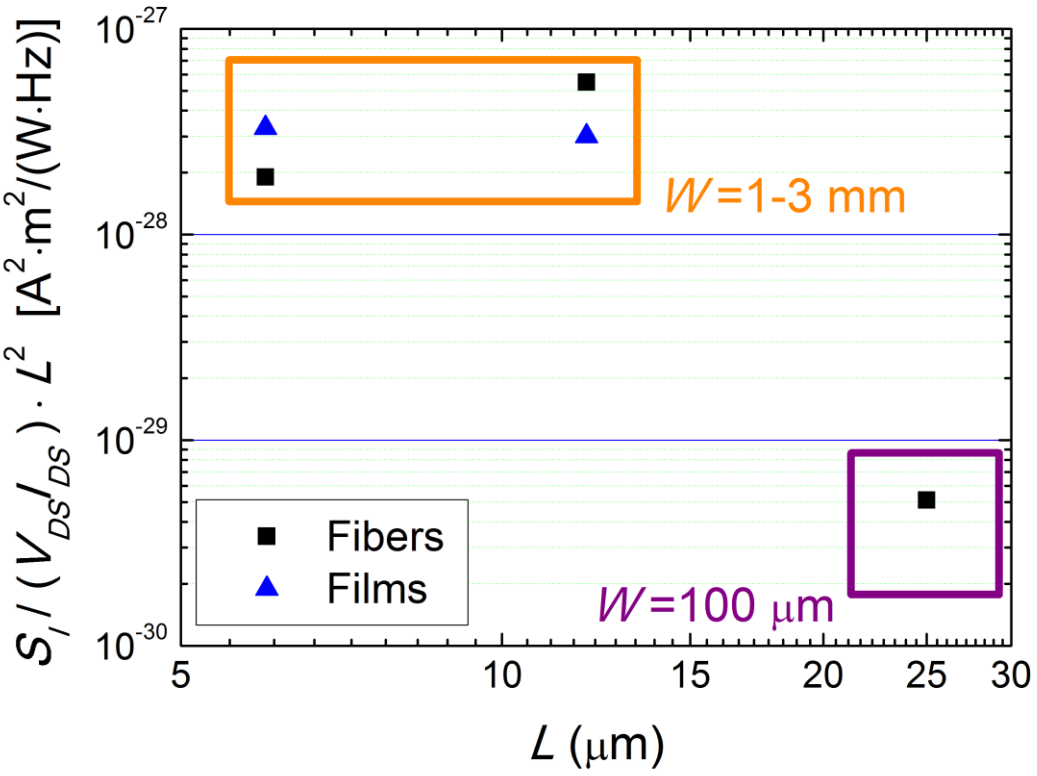

Figure S2. Comparison of the normalized noise level at 1 kHz and $V_{SD} \cdot I_D$ = 1 μW.

2. Effect of nanowire bending and cross-sectional inhomogeneities

The possible bending as well as the presence of inhomogeneous degrees of regioregularity and charge delocalization in the different cross-sectional regions of the polymer nanowire are described by considering a conductive fiber with $r_n = r_H + \delta r_H(x,y)$ for horizontal resistors, and $r_n = r_V + \delta r_V(x,y)$ for vertical resistors, where $\delta r_H(x,y)$ and $\delta r_V(x,y)$ are not random but dependent on the position along the transversal and longitudinal fiber axes (Fig. 4a). A similar choice is adopted for the variances associated with the time fluctuations of the elementary resistors. Since this description adds a

"deterministic" position-dependent component to the values of the resistances, we neglect the random component in their values in order to leave the model as simple as possible and with a reduced number of parameters. Contacts are assumed to be non-ideal, as explained in the main text and detailed in the next Section. Precisely, fiber bending or cross-sectional inhomogeneities are taken into account by considering a dependence of the resistors and of the variance of the resistance fluctuations on the distance from a given position ("bending center" of the nanowire) having coordinates $x = j_c$ and $y = i_c$, as schematized in Fig. S3a. This dependence is different along the transversal and the longitudinal axes of the nanowire. In detail:

$$r_{H,l}(j, i) = r_H + dr_{HL} |j - j_c| + dr_{HT} |i - i_c| \quad \text{(S1a)}$$

$$r_{V,l}(j, i) = r_V + dr_{VL} |j - j_c| + dr_{VT} |i - i_c| \quad \text{(S1b)}$$

$$\Delta_{H,l}(j, i) = \delta_H + \delta_{HL} |j - j_c| + \delta_{HT} |i - i_c| \quad \text{(S2a)}$$

$$\Delta_{V,l}(j, i) = \delta_V + \delta_{VL} |j - j_c| + \delta_{VT} |i - i_c| \quad \text{(S2b)}$$

where l=1,..,N_L, and l=1,..,N_W for horizontal (i.e., longitudinal) or vertical (i.e., transversal) resistors, respectively, r_H, r_V, δ_H, and δ_V are constants, dr_{HL} (δ_{HL}) and dr_{HT} (δ_{HT}) indicate the longitudinal and the transversal variation of horizontal resistances (variance of fluctuations), respectively, and dr_{VL} (δ_{VL}) and dr_{VT} (δ_{VT}) indicate the longitudinal and the transversal variation of vertical resistances (variance of fluctuations), respectively. The relative current noise calculated for various sets of parameters is shown in Fig. S3b. Although bending is found to slightly affect the Hooge constant, these effects do not lead to variations of the order of magnitude of α_H (inset of Fig. S3b).

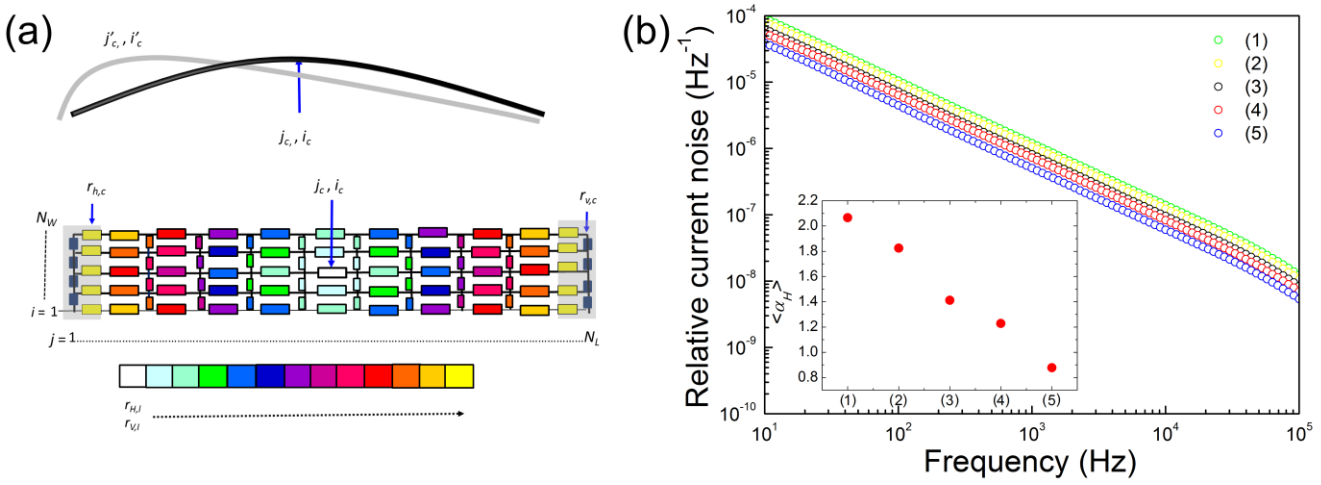

Fig. S3 (a) 2D network model of bent or cross-sectional irregular nanowires through fluctuating resistors. $x = j_c$ and $y = i_c$ are the coordinates of the nanowire "bending center". Colors in the network of resistors represent the different resistance values. (b) Resulting frequency dependence of S_I/I^2. Parameters: in all cases r_H=10^5 Ω, r_V=10^4 Ω, δ_H=6×10^9 Ω^2, δ_V=10^6 Ω^2 (i.e. same values as $r_{H,a}$, $r_{V,a}$, $\Delta_{H,a}$, and $\Delta_{V,a}$ in Fig. 4). The spectral densities denoted with (1) and (4) differ for the increments of the resistance variances, δ_{HT} and δ_{VT}, along the transversal axis, whereas curves (2) and (5) differ for the increment of the same quantities along the longitudinal axis, δ_{HL} and δ_{VL}. Curves (3) and (4) differ for the trasversal increments of the resistances, dr_{HT} and dr_{VT}, and curves (3) and (5) for the longitudinal increments of the resistances, dr_{HL} and dr_{VL}. Precisely (resistances in Ω, variances in Ω^2): $dr_{HL} = 6\times10^2$, $dr_{HT} = 1\times10^4$, $dr_{VL} = 6\times10^1$, $dr_{VT} = 1\times10^3$, $\delta_{HL} = 3\times10^9$, $\delta_{HT} = 1\times10^{11}$, $\delta_{VL} = 3\times10^4$, $\delta_{VT} = 1\times10^7$ (1); $dr_{HL} = 2\times10^3$, $dr_{HT} = 6\times10^3$, $dr_{VL} = 2\times10^2$, $dr_{VT} = 6\times10^2$, $\delta_{HL} = 3\times10^9$, $\delta_{HT} = 4\times10^{10}$, $\delta_{VL} = 3\times10^4$, $\delta_{VT} = 4\times10^5$ (2); $dr_{HL} = 6\times10^2$, $dr_{HT} = 6\times10^3$, $dr_{VL} = 60$, $dr_{VT} = 6\times10^2$, $\delta_{HL} = 3\times10^9$, $\delta_{HT} = 4\times10^{10}$, $\delta_{VL} = 3\times10^4$, $\delta_{VT} = 4\times10^5$ (3); $dr_{HL} = 6\times10^2$, $dr_{HT} = 1\times10^4$, $dr_{VL} = 60$, $dr_{VT} = 1\times10^3$, $\delta_{HL} = 3\times10^9$, $\delta_{HT} = 4\times10^{10}$, $\delta_{VL} = 3\times10^4$, $\delta_{VT} = 4\times10^5$ (4); $dr_{HL} = 2\times10^3$, $dr_{HT} = 6\times10^3$, $dr_{VL} = 2\times10^2$, $dr_{VT} = 6\times10^2$, $\delta_{HL} = 3\times10^9$, δ_{HT} =

4×10^{10}, $\delta_{VL} = 3\times10^{4}$, $\delta_{VT} = 4\times10^{5}$ (5). Inset: α_H values for the various set of parameters (1)-(5). For comparison, by taking the above reported values for r_H, r_V, δ_H and δ_V (common to all the sets 1-5) and $dr_{HL} = dr_{HT} = dr_{VL} = dr_{VT} = 0$ and $\delta_{HL} = \delta_{HT} = \delta_{VL} = \delta_{VT} = 0$ (i.e. no bending and perfectly homogeneous fiber) one obtains $\alpha_H = 0.1025$, supporting the conclusion that though bending can affect the noise level of the nanowire, these effects do not lead to large variations of α_H.

3. Modelization of the effect of non-ideal contacts on the noise of the nanofiber device.

We have investigated by numerical simulations the effects of non-ideal contacts, i.e. electrodes with not negligible resistance and resistance noise, on the electrical properties of the overall device (nanofiber plus contacts). To model these effects, we consider the $N_W \times N_L$ network made by N_T *regular resistors* of resistance r_n (describing the nanofiber), in contact with two lateral bars. Each bar is composed by $2N_W + 1$ resistors (*contact resistors*): $N_W + 1$ horizontal resistors of resistance $r_{h,c}$ and N_W vertical resistors of resistance $r_{v,c}$ (Fig. 5a). The horizontal contact resistors describe the effect of the disordered and high-resistivity regions at the interface between the metal and the nanofiber, whereas the vertical contact resistors are associated with the resistivity of the metallic region, thus it is reasonable to assume $r_{v,c} << r_{h,c}$. In conclusion, the overall device is simulated by a network of resistance $R_T \neq R_{fiber}$, made by $N_T + N_{cont}$ resistors, with $N_{cont} = 4N_W + 2$.

Here, as preliminary investigation, we neglect the possibility of non-homogeneous or asymmetrical contacts. Therefore, all the resistors $r_{h,c}$ composing the electrodes are taken equal, and the same assumption is considered for $r_{v,c}$. In any case the existence of dishomogeneities or differences in the electrical properties of the two electrodes can be easily accounted for in our model. Consistently

with our hypotheses, the noise of the contacts is described by assuming that contact resistors fluctuate with variances $\Delta_{h,c} \equiv \langle(\Delta r_{h,c})^2\rangle$ and $\Delta_{v,c} \equiv \langle(\Delta r_{v,c})^2\rangle$, equal for all horizontal and vertical resistors respectively. For good quality electrodes, one can assume $\Delta_{v,c} << \Delta_{h,c}$.

Moreover, contact resistors are characterized by a random value of the correlation time, τ_c, distributed in the same time interval of the regular resistors. The last assumption is equivalent to the hypothesis that the noise of the contacts does not affect the $1/f$ shape of the current noise power spectrum. Other assumptions concerning the correlations times (for example, τ_c distributed in a range of values different for regular and contact resistors), can be straightforwardly included in the model. This generalization would enable a study of the effect of the contacts on the shape of the noise power spectrum, which is left for further investigation.

Therefore, neglecting the effects of $r_{v,c}$ and $\Delta_{v,c,}$ at the simplest level of modelization the presence of non-ideal contacts is accounted for by the two parameters, $r_{h,c}$ and $\Delta_{h,c}$. In the following, we discuss their effects on the total device resistance, R_T, and on the strength of the flicker noise, as measured by α_H. Fig. S4 shows the dependence of R_T on $r_{h,c}$, where R_T is obtained by solving the $N_W \times N_L+1$ Kirchhoff's loop equations. Precisely, the resistance in Fig. S4 is calculated for the same network (8×100) considered in Fig. 4c, but in contact with two non-ideal electrodes according to the schematic representation of Fig. 5a. The total resistance R_T starts to depend on $r_{h,c}$ for $r_{V,a} < r_{h,c} < r_{H,b}$. This dependence becomes particularly significant for $r_{h,c} > r_{H,b}$. Finally, for $r_{h,c} >> r_{H,b}$, R_T is dominated by the resistance of the contacts associated with the fiber-metal interface.

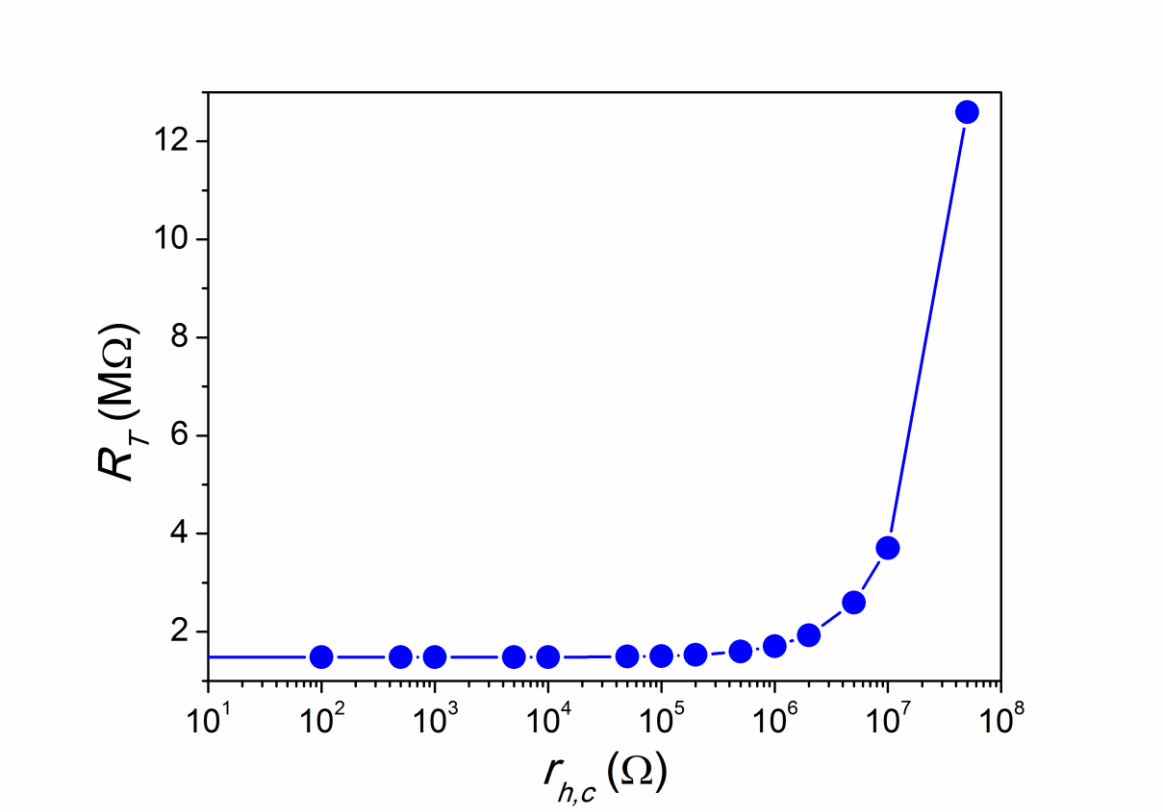

Figure S4. R_T vs. $r_{h,c}$ for a 8×100 network (same as in Fig. 4c, but in contact with non-ideal electrodes). $r_{v,c} = 0$.

We notice that the values of α_H obtained for different realizations of the statistical ensemble (nominally identical samples measured under identical external conditions) are scattered inside a certain range of values. Therefore, to clearly identify the dependence of α_H on $r_{h,c}$ or $\Delta_{h,c}$ (or on other parameters) we consider the ensemble average, $<\alpha_H>$, of the α_H values. For this reason, in Fig. 5b we show $<\alpha_H>$ vs. $r_{h,c}$. Fig. 5b clearly points out that:

(i) $<\alpha_H>$ starts to decrease upon increasing $r_{h,c}$ above a threshold value $\cong r_{V,a}$ (the smallest elementary resistance composing the nanofiber network);

(ii) the value of $<\alpha_H>$ for low $r_{h,c}$ strongly depends on $\Delta_{h,c}$ only in the case of rather noisy contacts, i.e. for $\Delta_{h,c} > \Delta_{H,b}$ (the highest resistance variance of the fluctuating resistors composing the nanofiber network), whereas it keeps the ideal-contact value for $\Delta_{h,c} < \Delta_{H,b}$.

(iii) $<\alpha_H>$ decreases strongly for $r_{h,c} > r_{H,b}$.

While features (i) and (ii) can be easily understood, the decrease of the current noise for increasing values of the contact resistance is more intriguing. To understand this behavior, one should consider that the value of $r_{h,c}$ (and thus of the contact resistance) strongly affects the distribution of local currents. In particular, increasing $r_{h,c}$ leads to sharper distributions of local currents i_n in the network (Fig. S5), as also shown by the smaller values of the root mean deviation (σ_i) of the local current distribution. For example, for the results shown in Fig. 5b and obtained for $\Delta_{h,c} = 10^{12}\ \Omega^2$, one has $\sigma_i \cong 0.98\ \mu A$ for $r_{h,c} = 10^2\ \Omega$ and $\sigma_i \cong 0.38\ \mu A$ for $r_{h,c} = 10^7\ \Omega$. The variance of current noise (thus also the spectral density of current noise) is strictly related to the fourth moment of the local current distribution,[S2,S3] which explains the reduction of $<\alpha_H>$ shown in Fig. 5b.

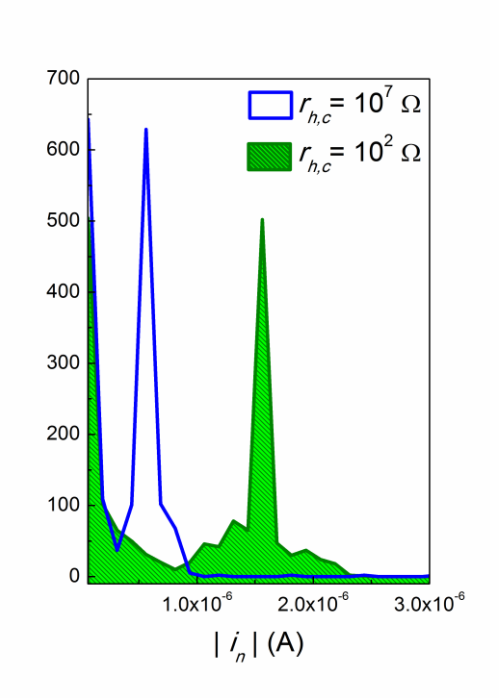

Figure S5. Distribution of local currents flowing in a 8×100 network for two different values of the elementary contact resistance, $r_{h,c}$ =10^2 Ω and $r_{h,c}$ =10^7 Ω. $\Delta_{h,c}$ =10^{12} Ω^2 in both cases. All other parameters are the same as in Fig. 5b.

References

(S1) Lai, Y.; Li H.; Kim, D. K.; Diroll, B. T., Murray, C. B.; Kagan, C. R.; Low-Frequency (1/f) Noise in Nanocrystal Field-Effect Transistors. *ACS Nano* **2014**, 9, 9664-9672.

(S2) Rammal, R.; Tannous, C.; Breton, P.; Tremblay, A. M. S. Flicker (1/f) Noise in Percolation Networks: A New Hierarchy of Exponents. *Phys. Rev. Lett.* **1985**, *54*, 1718-1721.

(S3) Stauffer, D.; Aharony, A. *Introduction to Percolation Theory*. London: Taylor and Francis 1991.